

ISSN: 0095-8972 (Print) 1029-0389 (Online) Journal homepage: <http://www.tandfonline.com/loi/gcoo20>


## Bis(imidazole) coordination polymers controlled by oxalate as an auxiliary ligand

Ya-Guang Sun, Jian Li, Jiang You, Ying Guo, Gang Xiong, Bao-Yi Ren, Li-Xin You, Fu Ding, Shu-Ju Wang, Francis Verpoort, Ileana Dragutan & Valerian Dragutan


To cite this article: Ya-Guang Sun, Jian Li, Jiang You, Ying Guo, Gang Xiong, Bao-Yi Ren, Li-Xin You, Fu Ding, Shu-Ju Wang, Francis Verpoort, Ileana Dragutan & Valerian Dragutan (2015) Bis(imidazole) coordination polymers controlled by oxalate as an auxiliary ligand, Journal of Coordination Chemistry, 68:7, 1199-1212, DOI: [10.1080/00958972.2015.1012072](https://doi.org/10.1080/00958972.2015.1012072)


To link to this article: <http://dx.doi.org/10.1080/00958972.2015.1012072>

 View supplementary material 

 Accepted author version posted online: 27 Jan 2015.  
Published online: 19 Feb 2015.

 Submit your article to this journal 

 Article views: 46

 View related articles 

 View Crossmark data 

 Citing articles: 1 View citing articles 

## Bis(imidazole) coordination polymers controlled by oxalate as an auxiliary ligand

YA-GUANG SUN\*†, JIAN LI†, JIANG YOU†, YING GUO†, GANG XIONG†, BAO-YI REN†, LI-XIN YOU†, FU DING†, SHU-JU WANG†, FRANCIS VERPOORT‡§, ILEANA DRAGUTAN¶ and VALERIAN DRAGUTAN¶

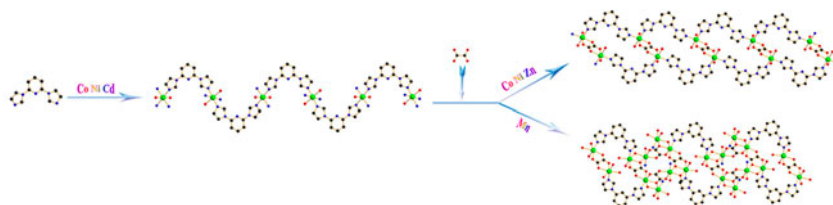
†Laboratory of Coordination Chemistry, Shenyang University of Chemical Technology, Shenyang, China

‡State Key Laboratory of Advanced Technology for Materials Synthesis and Processing, Faculty of Sciences, Department of Applied Chemistry, Center for Chemical and Material Engineering, Wuhan University of Technology, Wuhan, China

§Department of Inorganic and Physical Chemistry, Organometallics and Catalysis, Ghent University, Ghent, Belgium

¶Institute of Organic Chemistry “C. D. Nenitescu”, Romanian Academy, Bucharest, Romania

(Received 16 August 2013; accepted 20 January 2015)



In hydrothermal reactions, seven coordination polymers were synthesized. Single-crystal X-ray diffraction analysis revealed that compounds **1–3** possess 2-D networks, whereas compounds **4–6** involve two kinds of oxalate chains. The structure of **7** adopts a 3-D framework structure due to various bridging modes of the oxalate ligand. Magnetic studies have revealed that compounds **1**, **2**, **4**, **5**, and **7** exhibit strong antiferromagnetic coupling.

Seven coordination polymers  $\{[M(L)_2(H_2O)_2] \cdot (NO_3)_2\}_n$  ( $M = Co$  (**1**),  $Ni$  (**2**),  $Cd$  (**3**)) and  $[M(L)(ox)]_n$  ( $M = Co$  (**4**),  $Ni$  (**5**),  $Zn$  (**6**), and  $Mn$  (**7**)) have been synthesized ( $L = 2,6$ -bis(imidazol-1-yl)pyridine,  $ox = oxalate$ ) under hydrothermal conditions. Single-crystal X-ray diffraction analysis has revealed that **1–3** are isomorphous and possess 2-D networks, whereas **4–6** are isomorphous, but involve two kinds of oxalate chains. The structure of **7** is different from those of **4–6** due to various bridging modes of the oxalate ligand. Magnetic studies have revealed that **1**, **2**, **4**, **5**, and **7** exhibit strong antiferromagnetic coupling. Among these, **1** exhibits an interesting spin-canting phenomenon.

**Keywords:** Bis(imidazole); Auxiliary oxalate ligand;  $\pi$ - $\pi$  Stacking; Magnetic properties

\*Corresponding author. Email: [sunyaguang@syuct.edu.cn](mailto:sunyaguang@syuct.edu.cn)

## 1. Introduction

Rational design and advanced synthesis of coordination polymers have attracted the attention of chemists due to potential applications of such systems in catalysis, molecular adsorption, magnetism, nonlinear optics, luminescence, and molecular sensing [1, 2], as well as their intriguing structural motifs [3, 4]. As basic components of coordination polymers, ligands are indispensable, especially azole ligands, such as imidazole, pyrazole, triazole, and tetrazole, which represent a class of aromatic N-donor organic linkers [5–9]. In particular, imidazole-containing ligands, which are building blocks with two nitrogen donors oriented at an appropriate angle (*ca.* 135–145°) provide very rich structural chemistry different from those of other types of coordination polymers due to their variable bent coordination geometries [10]. Many research groups have investigated a variety of mono(imidazole) ligands, as small and simple organic ligands. For example, Zhang *et al.* established the first 3-D coordination polymer of  $[\text{Mn}_2(\text{IMDC})_2(\text{H}_2\text{O})_2]$  (IMDC = 4,5-imidazoledicarboxylate) containing left- and right-handed helical chains, in which weak antiferromagnetic exchange interactions exist between the neighboring  $\text{Mn}^{2+}$  ions [11]. Bis(imidazole) ligands linked by benzene, pyridine, and azoles have also been reported [12]. For instance, Wen *et al.* reported the fourfold interpenetration of identical  $[\text{Zn}_2(\text{SIP})(\text{bix})_3(\text{OH})_2\text{H}_2\text{O}]_n$  (SIP = 5-sulfoisophthalic acid monosodium salt, bix = 1,4-bis(imidazol-1-ylmethyl)benzene) frameworks, which displayed strong fluorescent emission [12(a)].

Oxalate as an auxiliary ligand, as the simplest multidentate organic connecting ligand, has attracted our attention because of its ability to bind strongly with metals in diverse connection modes. Use of oxalate has resulted in various interesting oxalate-containing structures, such as metal oxalate chains or metal oxalate networks [13–25].

Herein, we explore the possibility of employing the bis(imidazole) ligand L (L = 2,6-bis(imidazol-1-yl)pyridine) for the construction of a set of coordination polymers. Although this ligand has been described by other groups [26, 27], we obtained three coordination polymers,  $\{[\text{M}(\text{L})_2(\text{H}_2\text{O})_2] \cdot (\text{NO}_3)_2\}_n$  (M = Co (**1**), Ni (**2**), Cd (**3**)) that adopt 2-D wavelike networks. Further, by adding oxalate (ox) as an auxiliary ligand, we obtained four other polymers,  $[\text{M}(\text{L})(\text{ox})]_n$  (M = Co (**4**), Ni (**5**), Zn (**6**), and Mn (**7**)), which show diversified structures due to the cooperative interaction of the two ligands. Complexes **4–6** possess networks that contain a zip-like double chain, while **7** adopts a 3-D framework structure. Magnetic studies have revealed that **1**, **2**, **4**, **5**, and **7** exhibit strong antiferromagnetic coupling, with **1** showing an interesting spin-canting phenomenon.

## 2. Experimental

### 2.1. Materials and methods

All chemicals were obtained from commercial sources and used without purification. C, H, and N analyses were carried out on a Perkin–Elmer 240 elemental analyzer. IR spectra were recorded from 4000 to 400  $\text{cm}^{-1}$  on a Nicolet 470 spectrophotometer from samples in KBr pellets. Powder X-ray diffraction patterns of the samples were recorded on a Bruker D8 Advance X-ray diffractometer, employing Cu–K $\alpha$  radiation. Variable-temperature magnetic susceptibilities were measured on a Quantum Design MPMS-7 SQUID magnetometer. Diamagnetic corrections were made with Pascal’s constants for all constituent atoms.

## 2.2. Synthesis of 1–3

A mixture of  $M(\text{NO}_3)_2$  {0.1 mM ( $\text{Co}(\text{NO}_3)_2 \cdot 6\text{H}_2\text{O}$  0.0291 g,  $\text{Ni}(\text{NO}_3)_2 \cdot 3\text{H}_2\text{O}$  0.0290 g, and  $\text{Cd}(\text{NO}_3)_2 \cdot 4\text{H}_2\text{O}$  0.0308 g)}, L (0.0211 g, 0.1 mM), and water (10 mL) was sealed in a 25 mL Teflon reactor and kept under autogenous pressure at 150 °C for 3 days, then cooled to room temperature over 3 days. Pink block-shaped crystals of **1** were obtained in a yield of 64% (0.0410 g). Elemental Anal. Calcd (%) for  $\text{C}_{22}\text{H}_{22}\text{CoN}_{12}\text{O}_8$ : C, 41.19; H, 3.46; N, 26.20. Found: C, 41.27; H, 3.41; N, 26.22. Green block-shaped crystals of **2** were obtained in a yield of 60% (0.0472 g). Elemental Anal. Calcd (%) for  $\text{C}_{22}\text{H}_{22}\text{NiN}_{12}\text{O}_8$ : C, 41.21; H, 3.46; N, 26.21. Found: C, 41.29; H, 3.50; N, 26.11. Light-yellow block-shaped crystals of **3** were obtained in a yield of 66% (0.0457 g). Elemental Anal. Calcd (%) for  $\text{C}_{22}\text{H}_{22}\text{CdN}_{12}\text{O}_8$ : C, 38.03; H, 3.19; N, 24.19. Found: C, 38.10; H, 3.16; N, 24.23.

## 2.3. Synthesis of 4–6

A mixture of  $M(\text{NO}_3)_2$  {0.1 mM ( $\text{Co}(\text{NO}_3)_2 \cdot 6\text{H}_2\text{O}$  0.0291 g,  $\text{Ni}(\text{NO}_3)_2 \cdot 3\text{H}_2\text{O}$  0.0290 g, and  $\text{Zn}(\text{NO}_3)_2 \cdot 6\text{H}_2\text{O}$  0.0297 g)}, L (0.0211 g, 0.1 mM), oxalic acid (0.0126 g, 0.1 mM), and water (10 mL) was sealed in a 25 mL Teflon reactor and was kept under autogenous pressure at 150 °C for 4 days, then cooled to room temperature over 3 days. Pink block-shaped crystals of **4** were obtained in a yield of 64% (0.0229 g). Elemental Anal. Calcd (%) for  $\text{C}_{13}\text{H}_9\text{CoN}_5\text{O}_4$ : C, 43.59; H, 2.53; N, 19.55. Found: C, 43.62; H, 2.47; N, 19.58. Green block-shaped crystals of **5** were obtained in a yield of 58% (0.0254 g). Elemental Anal. Calcd (%) for  $\text{C}_{13}\text{H}_9\text{NiN}_5\text{O}_4$ : C, 43.62; H, 2.53; N, 19.56. Found: C, 43.65; H, 2.50; N, 19.51. Light-yellow block crystals of **6** were obtained in a yield of 57% (0.0207 g). Elemental Anal. Calcd (%) for  $\text{C}_{13}\text{H}_9\text{ZnN}_5\text{O}_4$ : C, 42.81; H, 2.48; N, 19.20. Found: C, 42.77; H, 2.53; N, 19.24.

## 2.4. Synthesis of 7

A mixture of  $\text{MnSO}_4 \cdot \text{H}_2\text{O}$  (0.0169 g, 0.1 mM), L (0.0422 g, 0.2 mM), oxalic acid (0.0252 g, 0.2 mM), and water (10 mL) was sealed in a 25 mL Teflon reactor and was kept under autogenous pressure at 150 °C for 4 days, then cooled to room temperature over 3 days. Yellow thin block-shaped crystals of **7** were obtained in a yield of 56% (0.0278 g). Elemental Anal. Calcd (%) for  $\text{C}_{15}\text{H}_9\text{Mn}_2\text{N}_5\text{O}_8$ : C, 42.81; H, 2.48; N, 19.20. Found: C, 42.77; H, 2.53; N, 19.24.

## 2.5. X-ray crystallography

Crystallographic data were collected on a Bruker SMART Apex CCD diffractometer using graphite-monochromated Mo- $K\alpha$  radiation (0.71073 Å) at 293 K in the  $\omega - 2\theta$  scan mode. An empirical absorption correction was applied to the data using *SADABS* [28]. The structures were solved by direct methods and refined by full-matrix least-squares method on  $F^2$  using the SHELXTL crystallographic software package [29]. All non-H atoms were refined anisotropically. The hydrogens were placed in calculated positions and refined using a riding mode. The crystallographic data, selected bond lengths, and angles for **1–7** are listed in tables S1 and S2 (see online supplemental material at <http://dx.doi.org/10.1080/00958972.2015.1012072>), respectively.

### 3. Results and discussion

#### 3.1. Structural description

Single-crystal X-ray diffraction results revealed that **1–3** belong to the  $P2_1/c$  space group. They are isomorphous (their crystal data are given in table S1), hence only the structure of **1**, as a representative example, will be discussed. As shown in figure 1, the asymmetric unit of **1** consists of one Co(II), two L, two coordinated waters, and two free nitrate ions. The Co(II) center is octahedrally coordinated by four nitrogens from four coordinated L and two waters. In the distorted octahedron, N(3B), N(3C), N(5), and N(5A) form a Co(II)-centered plane. The Co is at a center of symmetry, as is also seen in other compounds with bis(imidazole) ligands [30]. The Co–O bond distance is 2.116(3) Å and the Co–N bond distances are 2.163(3) and 2.148(3) Å, similar to those in  $[\text{Co}_3(\text{tmidc})_2\text{H}_2\text{O}]_4 \cdot (\text{H}_2\text{O})_4$  ( $\text{H}_3\text{tmidc} = 2-[(1H-1,2,4\text{-triazol-1-yl)methyl}]-1H\text{-imidazole-4,5-dicarboxylic acid}$ ) [31]. Detailed information is listed in table S2. In L, the imidazolyl rings are twisted from the pyridyl ring and the interplanar angles are  $9.90^\circ$  and  $25.55^\circ$ , respectively.

In **1**, Co(II) ions are bridged with different L ligands to form a 1-D zigzag chain [figure 2(a)], similar to the zigzag chain in  $\text{Zn(L)Br}_2 \cdot 0.25\text{H}_2\text{O}$  ( $\text{L} = 2,6\text{-bis(imidazol-1-yl)pyridine}$ ), reported by Chen's group [26]. Adjacent chains are connected by sharing metal ions, resulting in a further extension to a 2-D network structure [figure 2(b)]. The 2-D network forms a 3-D architecture through intermolecular C–H $\cdots$ O hydrogen-bonding interactions [C $\cdots$ O = 3.258(9), 3.332(7), 3.353(3), and 3.384(2) Å], involving the free nitrates [figure 2(c)]. There are also  $\pi$ – $\pi$  stacking interactions between imidazolyl rings with a centroid-to-centroid distance of 3.717 Å. Similar assemblies have been reported by other groups [26, 27], for which the inorganic metal salts  $\text{ZnX}_2$  ( $\text{X} = \text{Cl}, \text{Br}$ ) and  $\text{Co(NCS)}_2$ , respectively, were chosen to provide metal centers. In such cases, the inorganic anions were involved in coordination, acting as charge-balancing and space-filling agents in their compounds  $\text{Zn(L)Cl}_2 \cdot 0.5\text{H}_2\text{O}$ ,  $\text{Zn(L)Br}_2 \cdot 0.25\text{H}_2\text{O}$ , and  $\text{Co(NCS)}_2(\text{L})_2$  ( $\text{L} = 2,6\text{-bis(imidazol-1-yl)pyridine}$ ). Thus,  $\text{Zn(L)Cl}_2 \cdot 0.5\text{H}_2\text{O}$  and  $\text{Zn(L)Br}_2 \cdot 0.25\text{H}_2\text{O}$  possess *M*-helical and 1-D zigzag chain structures, respectively.  $\text{Co(NCS)}_2(\text{L})_2$  adopts a 2-D cylindrical tubular structure. For our work, we chose  $\text{Co(NO}_3)_2$  to generate metal centers and obtained a product with a 2-D network structure, but the nitrate ions were not involved in the coordination and only served to balance the charges [32].

Single-crystal X-ray diffraction studies revealed **4–6** to be isomorphous, with triclinic crystal systems. Here, only the structure of **4** will be discussed as a representative example. In **4**, each asymmetric unit contains one Co(II), one L, and one oxalate. As shown in

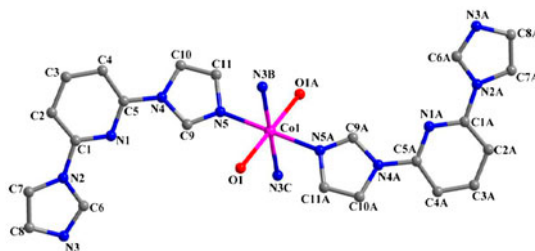


Figure 1. The structure of **1** at 30% thermal probability ellipsoids (free nitrate ions and hydrogens are omitted for clarity).

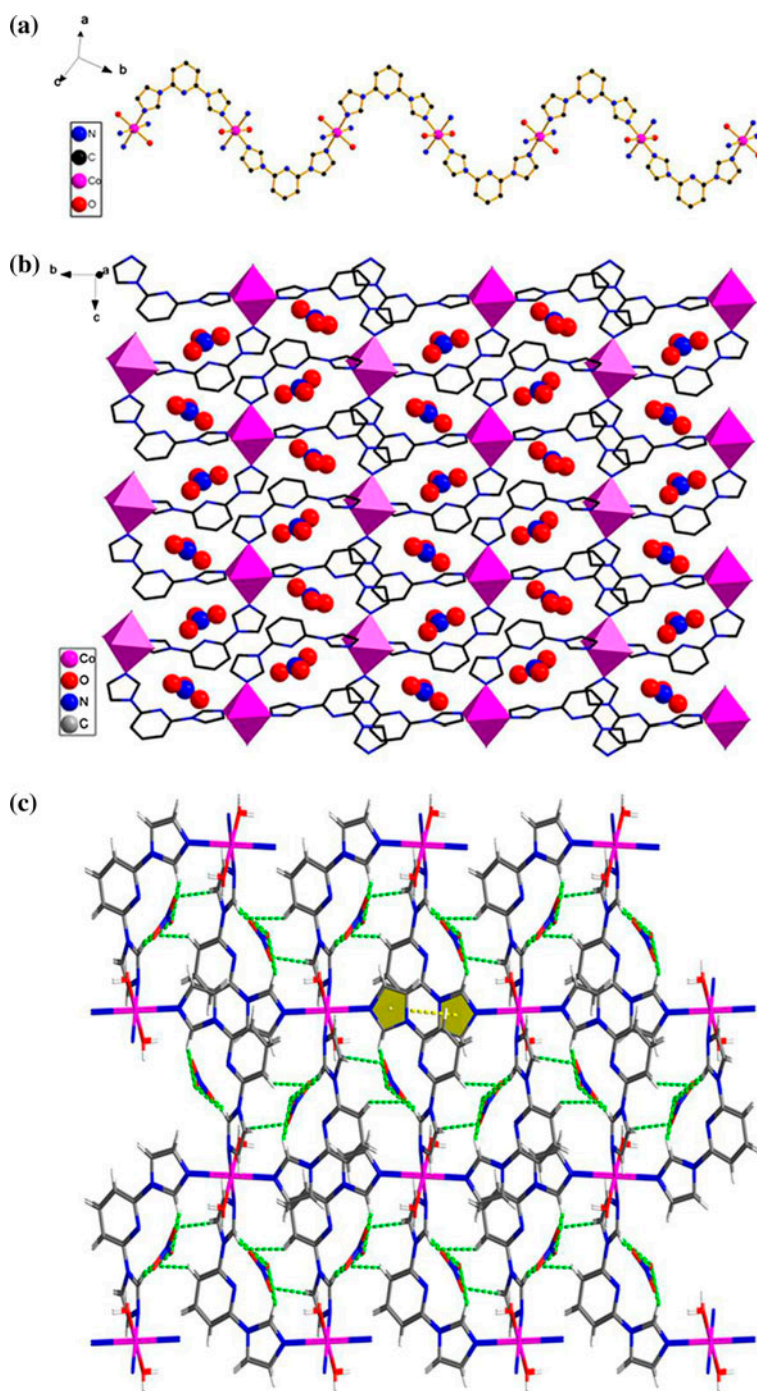


Figure 2. (a) Ball-and-stick representation of the 1-D chain in **1** (free nitrate ions and hydrogens are omitted for clarity). (b) Perspective view of the 2-D network structure in **1** (hydrogens are omitted for clarity). (c) The 3-D structure of **1** linked by C-H...O hydrogen bonds (the yellow rings represent  $\pi$ - $\pi$  stacking interactions) (see <http://dx.doi.org/10.1080/00958972.2015.1012072> for color version).

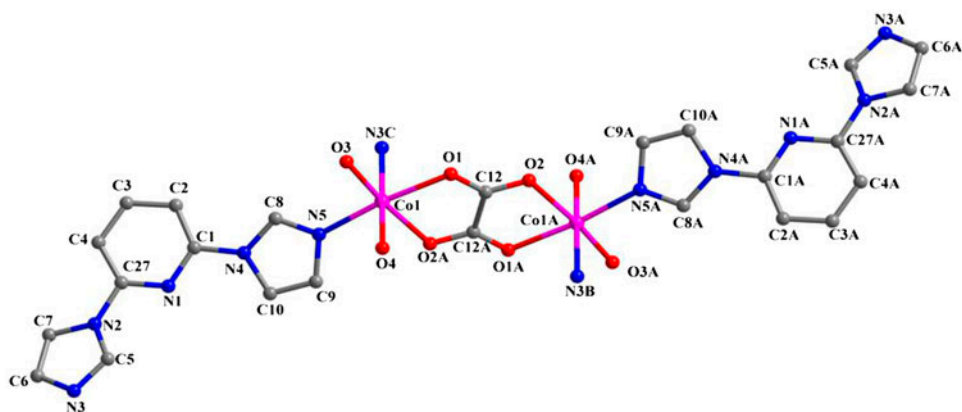


Figure 3. Coordination environment of **4** at 30% thermal probability ellipsoids (hydrogens are omitted for clarity).

figure 3, Co(II) is coordinated by two nitrogens and four oxygens, forming a distorted six-coordinate octahedral geometry. The N(3C), O(1), O(4), and N(5) make up the equatorial plane of the octahedral geometry and the Co(II) is at the midpoint of the equatorial plane. The Co–O bond lengths are 2.078–2.166 Å and the Co–N bond lengths are 2.123 and 2.140 Å. These values are similar to those in  $[\text{Co}_2(\text{ox})_2(\text{dchtpy})]_n \cdot 9n\text{H}_2\text{O}$  (dchtpy = 1a,4a-dihydroxy-1e,2e,4e,5e-tetra(4pyridyl)cyclohexane) [31], with Co–O bond lengths of 2.085–2.136 Å and Co–N bond length 2.104 Å. Detailed information is listed in table S2. In **L**, the imidazolyl rings are twisted from the pyridyl ring and their interplanar angles are 36.40° and 2.67°, respectively.

Compared with **1**, in the structure of **4**, because of the addition of oxalic acid, the coordination sites of water molecules are occupied by oxalate ligands instead. The 1-D single chain constructed from Co(II) and **L** is thereby assembled into a zip-like double chain [figure 4(a)]. The oxalates extend further along the direction of the *c*-axis, whereby the 1-D chain is extended into a 2-D ladder-type network. Another chain exists in the 2-D network, which is constructed from Co(II) ions and oxalate [figure 4(b)]. The 2-D ladder-type structure is different from the corrugated 2-D sheet structure of  $\{[\text{Zn}(\text{bpdc})(\text{bip})] \cdot 2\text{H}_2\text{O}\}_n$  constructed from biphenyl-4,4'-dicarboxylate and 3,5-bis(imidazol-1-yl)pyridine [33]. The form adopted mainly depends on the respective auxiliary ligands (biphenyl-4,4'-dicarboxylate and oxalic acid), thus indicating that auxiliary ligands play an important role in the formation of the compounds. The 2-D ladder-type networks are further extended to form 3-D structures via C–H···O hydrogen-bonding interactions [C···O = 3.395(3) and 3.365(3) Å]. Additionally, there are also  $\pi$ – $\pi$  stacking interactions between pyridyl rings with a centroid-to-centroid distance of 3.813 Å [figure 4(c)].

Single-crystal X-ray diffraction analysis revealed **7** to belong to a monoclinic crystal system with space group  $C2/c$ . Complex **7** differs from **4**–**6** because of the various coordination modes of oxalate [34]. As shown in figure 5, the asymmetric unit of **7** consists of one Mn(II), half of the **L**, and one oxalate. Oxalate O(1) links two Mn(II) ions in a bidentate bridging mode, giving a Mn–Mn distance of 3.625 Å, which is close to the distance of 3.64 Å in  $[\text{Mn}_2(\text{BPTCA})(\mu_2\text{-H}_2\text{O})_2]_n$  (BPTCA<sup>4-</sup> = 4,4'-bipyridine-2,2',6,6'-tetracarboxylate) [35]. Each Mn(II) shows a distorted octahedral geometric configuration and its six vertices

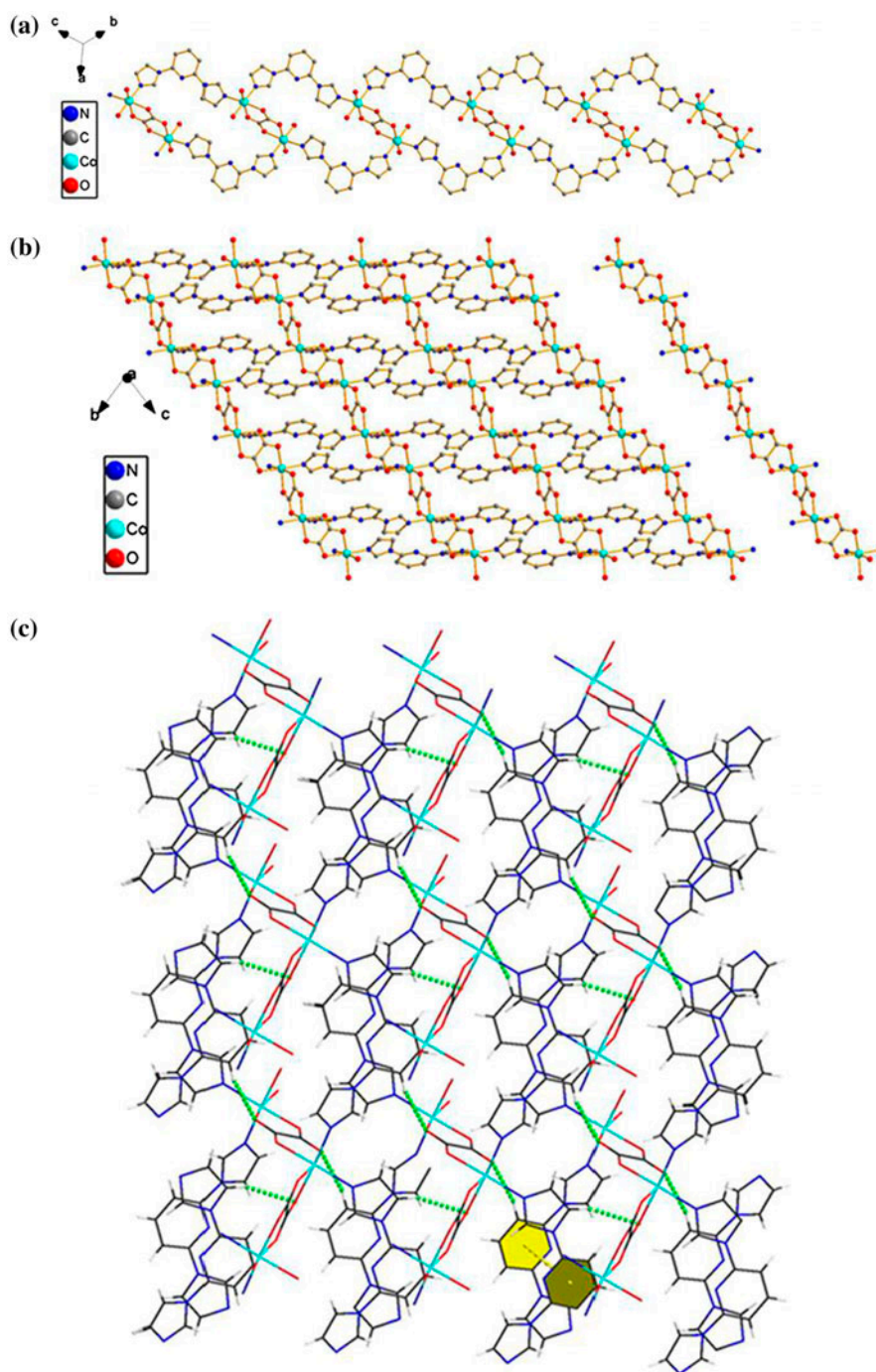


Figure 4. (a) Zip-like double chain with eight-coordinate metal ions linked by oxalate in **4** (hydrogens are omitted for clarity). (b) Perspective view of the 2-D ladder-type networks in **4** (hydrogens are omitted for clarity). (c) The 3-D structure of **4** linked by C-H...O hydrogen bonds (the yellow rings represent  $\pi$ - $\pi$  stacking interactions) (see <http://dx.doi.org/10.1080/00958972.2015.1012072> for color version).



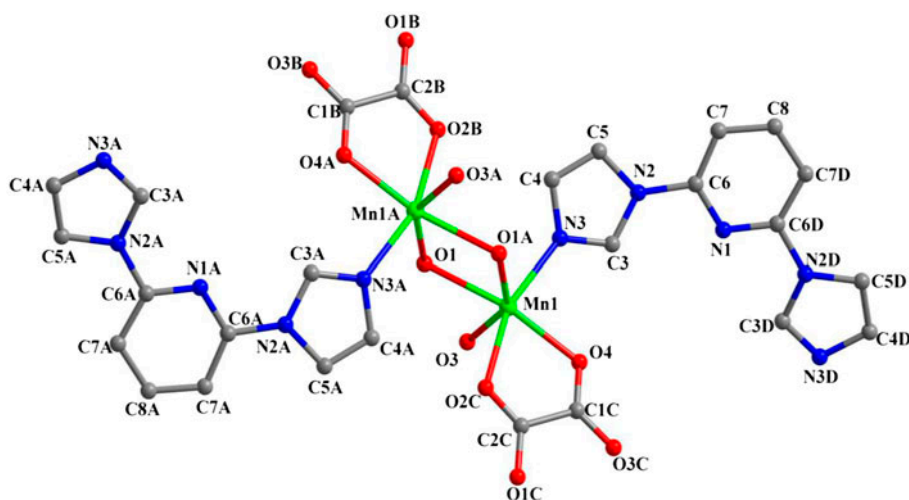


Figure 5. Coordination environment of **7** at 30% thermal probability ellipsoids (hydrogens are omitted for clarity).

are occupied by O(1), O(1A), O(2C), O(3), O(4), and N(3). The five oxygens are derived from oxalate ligands, and N(3) originated from L. O(1), O(1A), O(3), and O(4) are almost coplanar. The Mn–N bond distance is 2.186(2) Å and the average Mn–O bond distance is 2.209 Å, similar to those in [Mn(H<sub>3</sub>L)(ox)]·H<sub>2</sub>O (H<sub>3</sub>L = 1,3,5-tri(1*H*-imidazol-4-yl)benzene) [36].

As shown in figure 6(a), the binuclear Mn(II) ions are bridged by oxalate ligands to form a 1-D zigzag chain. The oxalate ligands also bridge adjacent chains, making the chains interwoven, resulting in the formation of a 2-D oxalate-bridged network [figure 6(b)]. A similar oxalate-bridged network of {NBu<sub>3</sub>(CH<sub>2</sub>COOH)}[MCr(ox)<sub>3</sub>]*n*H<sub>2</sub>O (Bu = *n*-butyl, M = Mn) has been reported [37]. However, the coordination mode of oxalates in **7** is (κ<sub>1</sub>-κ<sub>1</sub>-μ<sub>1</sub>)-(κ<sub>1</sub>-κ<sub>2</sub>-μ<sub>2</sub>)-μ<sub>3</sub> [scheme 1(a)], such that the Mn ions and oxalate ligands form a rectangular-based 2-D framework, whereas that in Ref. [37] is (κ<sub>1</sub>-κ<sub>1</sub>-μ<sub>1</sub>)-(κ<sub>1</sub>-κ<sub>1</sub>-μ<sub>1</sub>)-μ<sub>2</sub> [scheme 1(b)], such that the cationic and oxalate ligands form a honeycomb-like 2-D framework. The layers are parallel to the *bc* plane and the interlayer distance is 7.880 Å. The 2-D metal oxalate layers are further extended into a 3-D framework through L serving as a linker [figure 6(c)]. We used the PLATON program to calculate the total potential void volume in **7** and obtained a value of 41.53 Å<sup>3</sup>, which is equal to the volume of one water molecule.

### 3.2. Magnetic properties

The temperature-dependent susceptibilities of **1**, **2**, **4**, **5**, and **7** were measured from 300 to 2 K under a direct current of 1000 Oe. The corresponding  $\chi_m T$  versus *T* and  $\chi_m^{-1}$  versus *T* curves are depicted in figures 7–11. At 300 K, the  $\chi_m T$  value of **1** is 4.76 cm<sup>3</sup> K M<sup>-1</sup>, which is much higher than the theoretical value of 1.88 cm<sup>3</sup> K M<sup>-1</sup> calculated for one cobalt(II) center (<sup>4</sup>F<sub>9/2</sub>, *S* = 3/2). This behavior can be ascribed to strong spin-orbit coupling. Upon cooling,  $\chi_m T$  descends to a value of 4.11 cm<sup>3</sup> K M<sup>-1</sup> at 48 K and then increases to a value of 4.18 cm<sup>3</sup> K M<sup>-1</sup> at 35 K. The final minimum value of 3.59 cm<sup>3</sup> K M<sup>-1</sup> was observed at

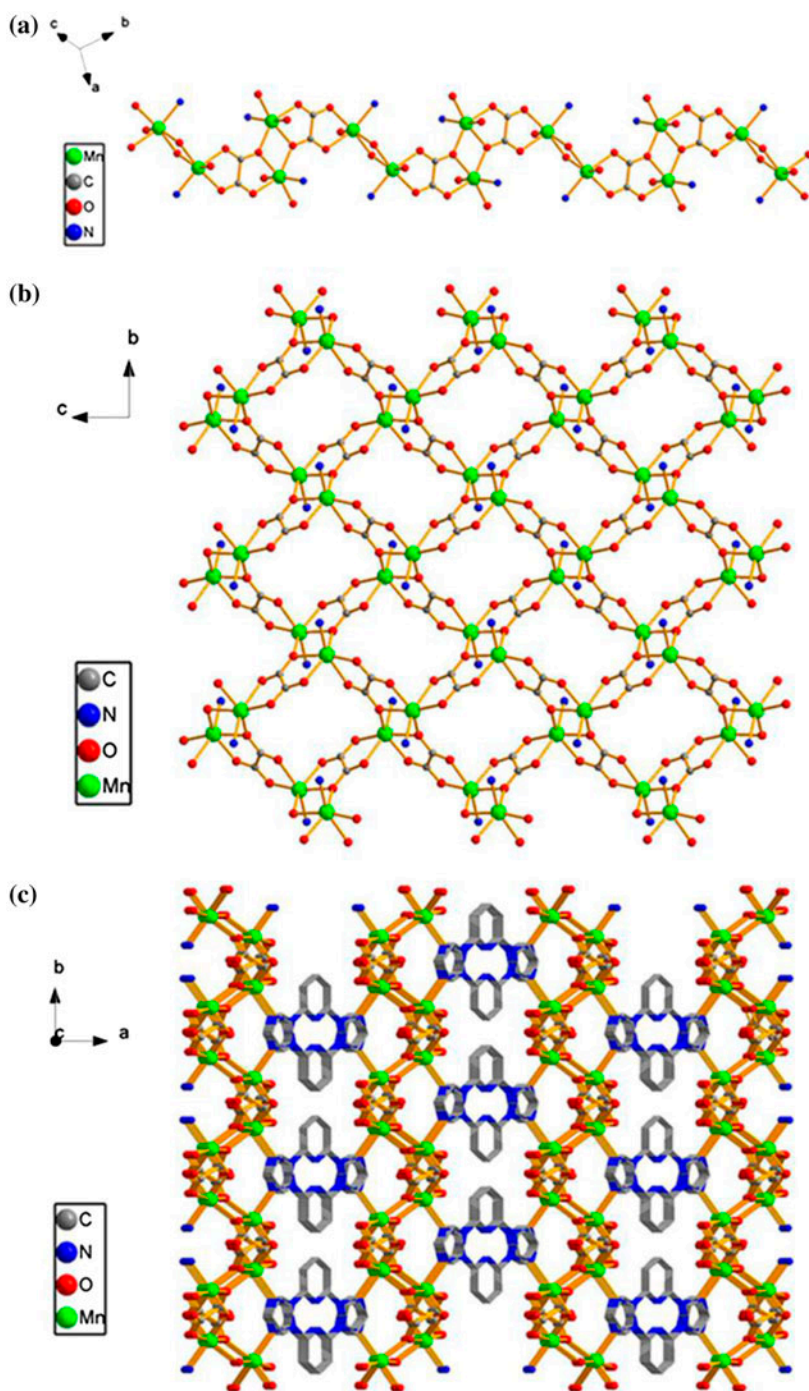


Figure 6. (a) Ball-and-stick representation of 1-D zigzag chain composed of oxalate in **7**. (b) Perspective view of the 2-D metal oxalate network in **7**. (c) Perspective view of the 3-D architecture in **7** (hydrogens are omitted for clarity).

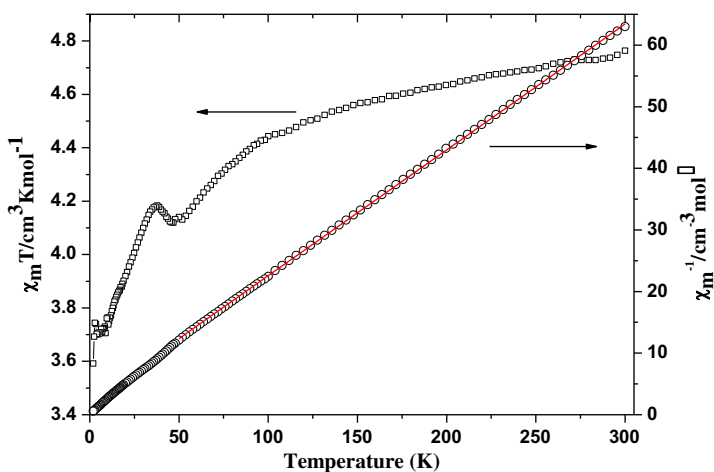


Figure 7.  $\chi_m T$  vs.  $T$  ( $\square$ ) and  $\chi_m^{-1}$  vs.  $T$  ( $\circ$ ) curves for **1**.

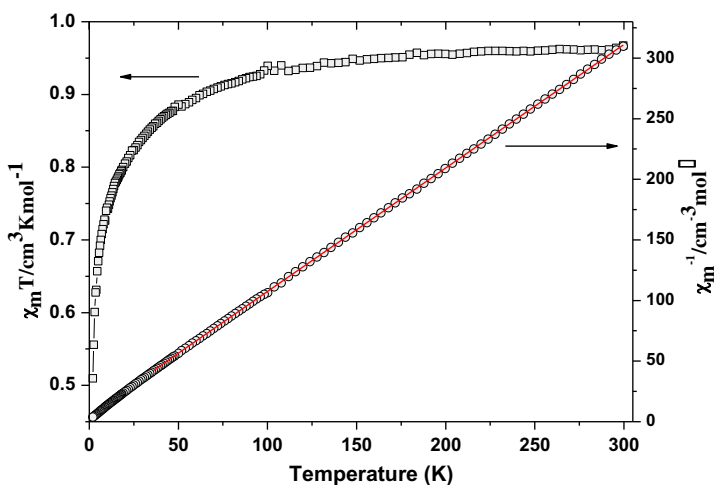


Figure 8.  $\chi_m T$  vs.  $T$  ( $\square$ ) and  $\chi_m^{-1}$  vs.  $T$  ( $\circ$ ) curves for **2**.

2 K. This curve shape clearly illustrates the existence of a spin-canting phenomenon [38]. Fitting of the curve of  $\chi_m^{-1}$  versus  $T$  above 50 K with the Curie–Weiss law resulted in a value of  $C = 4.89 \text{ cm}^3 \text{ K M}^{-1}$  and a negative  $\theta$  of  $-10.36 \text{ K}$ , indicating strong antiferromagnetic coupling. For **2**, the  $\chi_m T$  value is  $0.97 \text{ cm}^3 \text{ K M}^{-1}$ , which is close to the expected value of  $1.00 \text{ cm}^3 \text{ K M}^{-1}$  calculated on the basis of one nickel(II) center ( ${}^3F_4$ ,  $S = 1$ ) at room temperature. On lowering the temperature, the curve of  $\chi_m T$  versus  $T$  descends to a minimum value at 2 K in the form of a parabola. The  $\chi_m^{-1}$  versus  $T$  curve for **2** was fitted using the Curie–Weiss law with a Curie constant of  $0.98 \text{ cm}^3 \text{ K M}^{-1}$  and a negative  $\theta$  of  $-5.55 \text{ K}$ . The trends in the curve and the negative  $\theta$  value suggest that there is strong antiferromagnetic coupling in **2**. The occurrence of spin-canting is usually caused by single-ion

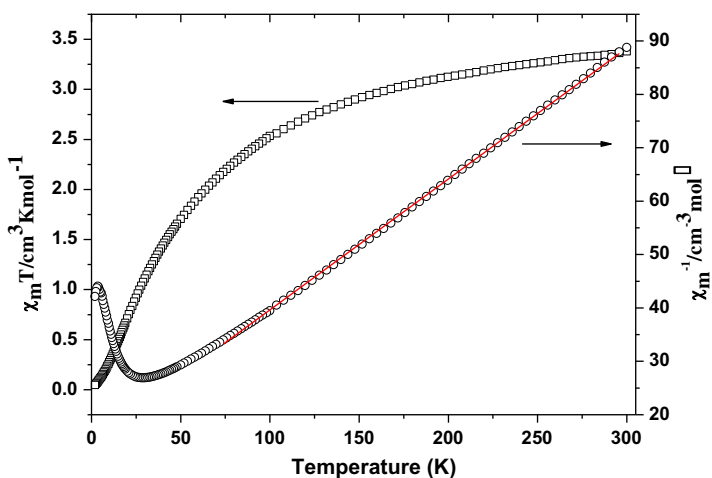


Figure 9.  $\chi_m T$  vs.  $T$  ( $\square$ ) and  $\chi_m^{-1}$  vs.  $T$  ( $\circ$ ) curves for **4**.

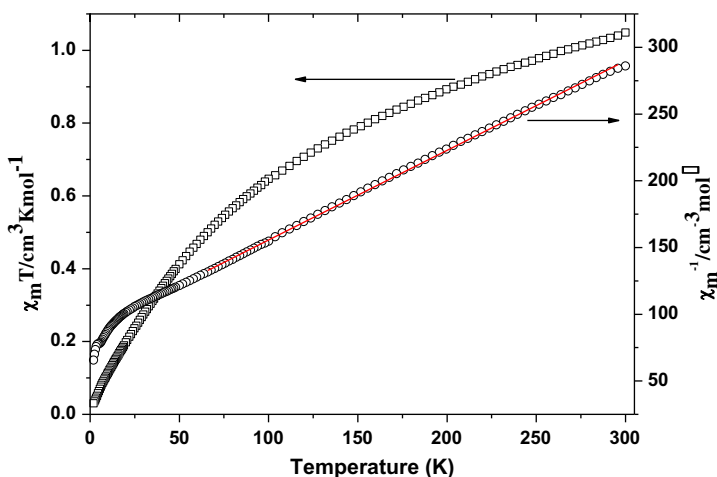


Figure 10.  $\chi_m T$  vs.  $T$  ( $\square$ ) and  $\chi_m^{-1}$  vs.  $T$  ( $\circ$ ) curves for **5**.

magnetic anisotropy and/or antisymmetric magnetic exchange [39]. For **1** and **2**, there is only one crystallographically independent spin center, and the asymmetric magnetic exchange is expected to be small. Therefore, the local anisotropy mainly determines the presence of the spin-canting phenomenon in the two isomorphous compounds. Co(II) cores are much more anisotropic than Ni(II), hence the spin-canting phenomenon can often be found in Co(II) complexes, but not in their Ni(II) homologues [39]. This seems to be the case in **1** and **2**.

At room temperature, the  $\chi_m T$  values of **5** and **7** are 1.048 and 8.01  $\text{cm}^3 \text{K M}^{-1}$ , respectively, which are close to the expected values of 1.00 and 8.7  $\text{cm}^3 \text{K M}^{-1}$  calculated on the basis of one nickel(II) center ( $^3F_4$ ,  $S = 1$ ) and two manganese(II) centers ( $^6S_{5/2}$ ,  $S = 5/2$ ).

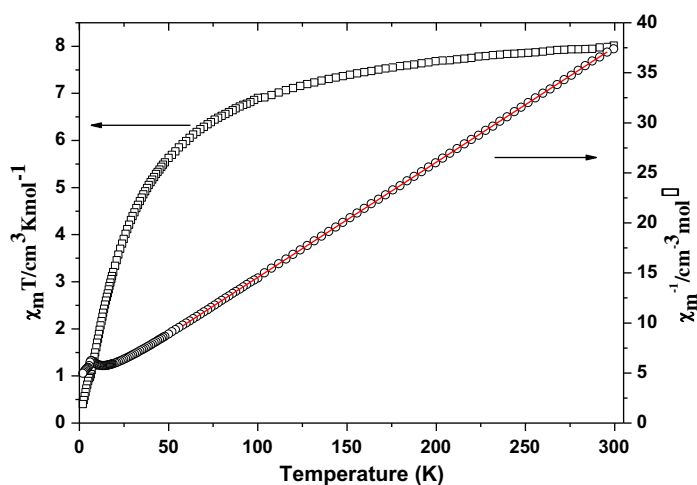
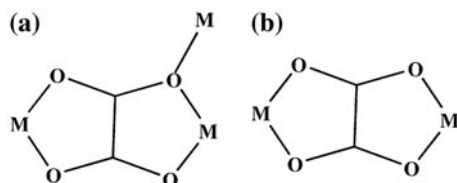


Figure 11.  $\chi_m T$  vs.  $T$  ( $\square$ ) and  $\chi_m^{-1}$  vs.  $T$  ( $\circ$ ) curves for **7**.



Scheme 1. The coordination modes of oxalate.

However, the  $\chi_m T$  value of **4** is  $3.38 \text{ cm}^3 \text{ K M}^{-1}$ , which is much higher than the theoretical value of  $1.88 \text{ cm}^3 \text{ K M}^{-1}$  calculated on the basis of one cobalt(II) ( $^4\text{F}_{9/2}$ ,  $S = 3/2$ ); this may be ascribed to strong spin-orbit coupling. On lowering the temperature, the curves of  $\chi_m T$  versus  $T$  for **4**, **5**, and **7** descend to minimum values at 2 K in the form of a parabola. The  $\chi_m^{-1}$  versus  $T$  curves for **4**, **5**, and **7** were fitted using the Curie–Weiss law, giving Curie constants of 4.07, 1.49, and  $8.67 \text{ cm}^3 \text{ K M}^{-1}$  and negative  $\theta$  values of  $-61.49$ ,  $-131.98$ , and  $-26.71 \text{ K}$ , respectively. The trends in the curves and the negative  $\theta$  values suggest that there is strong antiferromagnetic coupling in the structures of **4**, **5**, and **7**. This strong antiferromagnetic coupling appears to be mainly induced by the chelating oxalate ligands [40].

#### 4. Conclusion

Seven complexes containing 2,6-bis(imidazol-1-yl)pyridine have been synthesized. X-ray analyses revealed that **1–3** are isomorphous and adopt 2-D networks. Complexes **4–7** were constructed by employing oxalic acid as an auxiliary ligand, and of these **4–6** involve two kinds of chains. Various bridging modes of the oxalate ligands resulted in the structure of **7**,

which is distinct from those of **4–6**. Magnetic susceptibility measurements of **1**, **2**, **4**, **5**, and **7** have revealed the existence of strong antiferromagnetic coupling. Among these, **1** exhibits an interesting spin-canting phenomenon, which is mainly due to the fact that Co<sup>II</sup> displays an inherent anisotropy.

## Acknowledgements

This work was conducted in the framework of a project sponsored by the Natural Science Foundation of China (No. 21071100), the Distinguished Professor Project of Liaoning province and the Doctor Scientific Startup Foundation of Liaoning Province (No. 20111046). F.V. acknowledges the Chinese Central Government for an “Expert of the State” position in the program of “Thousand talents” and is grateful to Wuhan University of Technology for financial support. I.D. and V.D. acknowledge support from the Institute of Organic Chemistry “C.D. Nenitzescu” of the Romanian Academy.

## References

- [1] (a) L.E. Kreno, K. Leong, O.K. Farha, M. Allendorf, R.P. Van Duyne, J.T. Hupp. *Chem. Rev.*, **112**, 1105 (2012); (b) E. Coronado, G.M. Espallargas. *Chem. Soc. Rev.*, **42**, 1525 (2013); (c) J. Liu, P.K. Thallapally, B.P. McGrail, D.R. Brown, J. Liu. *Chem. Soc. Rev.*, **41**, 2308 (2012); (d) Y.J. Cui, Y.F. Yue, G.D. Qian, B.L. Chen. *Chem. Rev.*, **112**, 1126 (2012); (e) L.Q. Ma, C.D. Wu, M.M. Wanderley, W.B. Lin. *Angew. Chem. Int. Ed.*, **49**, 8244 (2010); (f) D. Farrusseng, S. Aguado, C. Pinel. *Angew. Chem. Int. Ed.*, **48**, 7502 (2009).
- [2] (a) J.R. Li, R.J. Kuppler, H.C. Zhou. *Chem. Soc. Rev.*, **38**, 1477 (2009); (b) C.G. Silva, A. Corma, H. García. *J. Mater. Chem.*, **20**, 3141 (2010); (c) Z.J. Zhang, Y.G. Zhao, Q.H. Gong, Z. Li, J. Li. *Chem. Commun.*, **49**, 653 (2013); (d) Z. Ni, A. Yassar, T. Antoun, O.M. Yaghi. *J. Am. Chem. Soc.*, **127**, 12752 (2005); (e) S.N. Wang, H. Xing, Y.Z. Li, J.F. Bai, Y. Pan, M. Scheer, X.Z. You. *Eur. J. Inorg. Chem.*, **15**, 3041 (2006).
- [3] (a) N. Stock, S. Biswas. *Chem. Rev.*, **112**, 933 (2012); (b) Q.X. Yang, X.Q. Chen, Z.J. Chen, Y. Hao, Y.Z. Li, Q.G. Lu, H.G. Zheng. *Chem. Commun.*, **48**, 10016 (2012); (c) Z.L. Wang, W.H. Fang, G.Y. Yang. *Chem. Commun.*, **46**, 8216 (2010).
- [4] G.P. Yong, S. Qiao, Y. Xie, Z.Y. Wang. *Eur. J. Inorg. Chem.*, **22**, 4483 (2006).
- [5] S.S. Chen, M. Chen, S. Takamizawa, M.S. Chen, Z. Su, W.Y. Sun. *Chem. Commun.*, **47**, 752 (2010).
- [6] F. Salles, G. Maurin, C. Serre, P.L. Llewellyn, C. Knöfel, H.J. Choi, Y. Filinchuk, L. Oliviero, A. Vimont, J.R. Long, G. Férey. *J. Am. Chem. Soc.*, **132**, 13782 (2010).
- [7] (a) J.P. Zhang, Y.Y. Lin, X.C. Huang, X.M. Chen. *Chem. Commun.*, **10**, 1258 (2005); (b) J.P. Zhang, Y.Y. Lin, X.C. Huang, X.M. Chen. *Cryst. Growth Des.*, **6**, 519 (2006).
- [8] X.L. Tong, D.Z. Wang, T.L. Hu, W.C. Song, Y. Tao, X.H. Bu. *Cryst. Growth Des.*, **9**, 2280 (2009).
- [9] W.L. Zhang, Y.Y. Liu, J.F. Ma, H. Jiang, J. Yang, G.J. Ping. *Cryst. Growth Des.*, **8**, 1250 (2008).
- [10] J.P. Zhang, Y.B. Zhang, J.B. Lin, X.M. Chen. *Chem. Rev.*, **112**, 1001 (2012).
- [11] M.B. Zhang, Y.M. Chen, S.T. Zheng, G.Y. Yang. *Eur. J. Inorg. Chem.*, **7**, 1423 (2006).
- [12] (a) L.L. Wen, Y.Z. Li, Z.D. Lu, J.G. Lin, C.Y. Duan, Q.J. Meng. *Cryst. Growth Des.*, **6**, 530 (2006); (b) C.W. Glynn, M.M. Turnbull. *Inorg. Chim. Acta*, **332**, 92 (2002); (c) Y. Qi, F. Luo, Y. Che, J. Zheng. *Cryst. Growth Des.*, **8**, 606 (2008); (d) W.G. Yuan, F. Xiong, H.L. Zhang, W. Tang, S.F. Zhang. *CrystEngComm*, **16**, 7701 (2014).
- [13] R.Q. Zhong, R.Q. Zou, D.S. Pandey, T. Kiyobayashi, Q. Xu. *Inorg. Chem. Commun.*, **11**, 951 (2008).
- [14] S. Decurtins, H.W. Schmalle, P. Schnewly, J. Ensling, P. Guetlich. *J. Am. Chem. Soc.*, **116**, 9521 (1994).
- [15] Q.H. Pan, J.Y. Li, Q. Chen, Y.D. Han, Z. Chang, W.C. Song, X.H. Bu. *Microporous Mesoporous Mater.*, **132**, 453 (2010).
- [16] E. Jeanneau, N. Audebrand, D. Louër. *Chem. Mater.*, **14**, 1187 (2002).
- [17] Y. Liu, G. Li, X. Li, Y. Cui. *Angew. Chem. Int. Ed.*, **46**, 6301 (2007).
- [18] P.A. Prasad, S. Neeraj, S. Natarajan, C.N.R. Rao. *Chem. Commun.*, **14**, 1251 (2000).
- [19] R. Vaidhyanathan, S. Natarajan, A.K. Cheetham, C.N.R. Rao. *Chem. Mater.*, **11**, 3636 (1999).
- [20] R. Vaidhyanathan, S. Natarajan, C.N.R. Rao. *Chem. Mater.*, **13**, 185 (2001).
- [21] M. Dan, C.N.R. Rao. *Angew. Chem. Int. Ed.*, **45**, 281 (2006).
- [22] R. Vaidhyanathan, S. Natarajan, C.N.R. Rao. *Inorg. Chem.*, **41**, 4496 (2002).
- [23] U. García-Couceiro, O. Castillo, A. Luque, J.P. García-Terán, G. Beobide, P. Román. *Cryst. Growth Des.*, **6**, 1839 (2006).

- [24] H. Okawa, A. Shigematsu, M. Sadakiyo, T. Miyagawa, K. Yoneda, M. Ohba, H. Kitagawa. *J. Am. Chem. Soc.*, **131**, 13516 (2009).
- [25] Q.H. Pan, Q. Chen, W.C. Song, T.L. Hu, X.H. Bu. *CrystEngComm*, **12**, 4198 (2010).
- [26] C.Y. Chen, P.Y. Cheng, H.H. Wu, H.M. Lee. *Inorg. Chem.*, **46**, 5691 (2007).
- [27] (a) S.U. Son, K.H. Park, B.Y. Kim, Y.K. Chung. *Cryst. Growth Des.*, **3**, 507 (2003); (b) J.Y. Lee, C.Y. Chen, H.M. Lee, E. Passaglia, F. Vizza, W. Oberhauser. *Cryst. Growth Des.*, **11**, 1230 (2011).
- [28] G.M. Sheldrick. *Program SADABS: Area-Detector Absorption Correction*, Göttingen University, Göttingen (1996).
- [29] G.M. Sheldrick. *SHELXL-97, Program for X-ray Crystal Structure Refinement*, Göttingen University, Göttingen (1997).
- [30] W. Zhang, L.J. Hao. *J. Coord. Chem.*, **66**, 2110 (2013).
- [31] H.Q. Hao, Z.J. Lin, S. Hu, W.T. Liu, Y.Z. Zheng, M.L. Tong. *CrystEngComm*, **12**, 2225 (2010).
- [32] P.F. Shi, G. Xiong, B. Zhao, Z.Y. Zhang, P. Cheng. *Chem. Commun.*, **49**, 2338 (2013).
- [33] J.K. Xu, X.C. Sun, C.X. Ju, J. Sheng, F. Wang, M. Sun. *J. Coord. Chem.*, **66**, 2541 (2013).
- [34] X. Han, X.X. Wang, G.H. Jin, X.G. Meng. *J. Coord. Chem.*, **66**, 800 (2013).
- [35] Z.S. Bai, Z.P. Qi, Y. Lu, Q. Yuan, W.Y. Sun. *Cryst. Growth Des.*, **8**, 1924 (2008).
- [36] S.S. Chen, Z.H. Chen, J. Fan, T. Okamura, Z.S. Bai, M.F. Lv, W.Y. Sun. *Cryst. Growth Des.*, **12**, 2315 (2012).
- [37] (a) M. Sadakiyo, H. Okawa, A. Shigematsu, M. Ohba, T. Yamada, H. Kitagawa. *J. Am. Chem. Soc.*, **134**, 5472 (2012); (b) X.J. Zhang, Y.H. Xing, C.G. Wang, J. Han, J. Li, M.F. Ge, X.Q. Zeng, S.Y. Niu. *Inorg. Chim. Acta*, **362**, 1058 (2009); (c) M. Jiang, Y.T. Li, Z.Y. Wu. *J. Coord. Chem.*, **65**, 1858 (2012).
- [38] X.Y. Wang, L. Wang, Z.M. Wang, G. Su, S. Gao. *Chem. Mater.*, **17**, 6369 (2005).
- [39] (a) J.R. Li, Q. Yu, Y. Tao, X.H. Bu, J. Ribas, S.R. Batten. *Chem. Commun.*, **22**, 2290 (2007); (b) H.P. Jia, W. Li, Z.F. Ju, J. Zhang. *Chem. Commun.*, **3**, 371 (2008); (c) F.P. Huang, J.L. Tian, D.D. Li, G.J. Chen, W. Gu, S.P. Yan, X. Liu, D.Z. Liao, P. Cheng. *CrystEngComm*, **12**, 395 (2010).
- [40] (a) C.R. Li, S.L. Li, X.M. Zhang. *Cryst. Growth Des.*, **9**, 1702 (2009); (b) Z.M. Duan, Y. Zhang, B. Zhang, F.L. Pratt. *Inorg. Chem.*, **48**, 2140 (2009).